

## Analysis of Aperture Field Uniformity for Biological Experiments

Honglong Cao<sup>1</sup>, Xueguan Liu<sup>1</sup>, Fenju Qin<sup>2</sup>, and Heming Zhao<sup>1, \*</sup>

**Abstract**—The uniformity of the incident electromagnetic radiofrequency fields (RF) is an import factor that can influence the results in biological *in vivo* and/or *in vitro* exposure experiments using animals and humans or their cells. The International Electrotechnical Commission (IEC) has published IEC 61000-4-20 standard which defined field uniformity criteria for emission and immunity testing in a defined region in transverse electromagnetic (TEM) waveguides. In this paper, we present a numerical analysis method to determine aperture field uniformity in biological experiments according to IEC 61000-4-20:2010 standard. With the numerical analysis method, the uniformity of electromagnetic field can be analyzed in Cartesian coordinates system by aperture-field method (AFM). Then, with the simultaneous application of AFM and the field uniformity criteria defined by IEC 61000-4-20:2010, the two functions can be programmed to evaluate the field uniformity in region of interest (ROI) which can then be meshed into the given observation points where biological examples are exposed to RF. At the specified position of ROI along  $z$  far from the aperture of the WR-430 rectangular open-ended waveguide, the field and the minimum uniform distances vs. frequencies can be calculated by AFM. Thus, the results of the numerical analysis method can be applied to design the exposure setups for biological experiments with the field uniformity required in ROI.

### 1. INTRODUCTION

Over the past several decades, wireless communication technologies have undergone rapid development and deployment into our daily lives. In recent two decades, cell phones, Bluetooth earphones and other WLAN/WIFI devices have become essential commodities for many people. Furthermore, implantable wireless medical devices are increasingly used to transmit and record real-time/store physiological data such as body temperature, blood pressure, and cardiac functions [1–4]. While people are benefitting from these wireless communication devices, the health effects from exposure to radiofrequency fields (RF) emitted from such devices have become a cause for concern. Many *in vivo* and *in vitro* experiments have been conducted, and the results reported are controversial and unclear whether or not RF exposure causes biological effects [5–8]. The absence of well-characterized and described RF exposure conditions for replication/confirmation studies may have been one of reasons for these conflicting results [9]. In terms of RF dosimetry, the field strength, uniformity of incident fields and specific absorption rate (SAR) are extremely important to determination/replication/confirmation of the biological effects of *in vivo* or *in vitro* exposure to RF. The distribution of SAR is also influenced by the uniformity of the incident fields. Therefore, RF field uniformity is a fundamental part in well-characterized conditions for RF exposure in biological experiments. For example, in animal experiments, the exposure setup should be designed with a field distribution as uniform as possible. The rectangular waveguide in which electromagnetic field is the fundamental  $TE_{10}$  propagation mode was demonstrated to provide a satisfactory field uniformity of at 1.95 Hz [10, 11]. The International Electrotechnical Commission (IEC) defined field uniformity criteria and published a standard, IEC 61000-4-20 which describes a

---

Received 13 November 2017, Accepted 2 February 2018, Scheduled 14 February 2018

\* Corresponding author: Heming Zhao (hmzhao@suda.edu.cn).

<sup>1</sup> School of Electronic & Information Engineering, Soochow University, Suzhou 215006, China. <sup>2</sup> Department of Biological Science and Technology, Suzhou University of Science and Technology, Suzhou 215009, China.

test method to evaluate the field uniformity in a defined area in Transverse Electromagnetic (TEM) Waveguide [12]. With the rapid development of computer technologies, the field uniformity can be numerically evaluated, and then the minimum uniform distance can be applied to improve the field uniformity in the region of interest (ROI) in the exposure setup according to IEC 61000-4-20 standard when the exposure setup is designed.

In this paper, we propose a numerical analysis method to evaluate the aperture field uniformity in the region of interest (ROI) where biological examples are placed and exposed to RF according to IEC 61000-4-20:2010 standard. (1) We will recommend IEC 61000-4-20:2010 standard for how to test and evaluate the field uniformity of ROI. (2) The rectangular open-ended waveguide model for the exposure setup is discussed where the electromagnetic field of ROI is derived by Aperture Field Method (AFM) in the Cartesian coordinates system. (3) We will derive reasonable formulas for constraint of field uniformity in ROI according to AFM and IEC 61000-4-20 standard. (4) We programm software to numerically analyze the field uniformity of ROI by the constraint formulas as derived above. (5) The minimum uniform position of ROI, far from the rectangular aperture, required to design the most optimal exposure setup is discussed.

## 2. FIELD UNIFORMITY CRITERIA

The International Standard IEC 61000-4-20 was published firstly in 2003, and the second edition was revised in 2010 about emission and immunity testing in transverse electromagnetic (TEM) waveguides. This standard propose field uniformity criteria and a test method to investigate the field uniformity of a defined area called ROI, where the biological examples are exposed to RF. According to IEC 61000-4-20:2010, the electromagnetic field of ROI should be verified as TEM mode and homogeneity. Therefore, the magnitude of electric field is measured to evaluate whether or not the specified filed uniformity criteria are fulfilled in the given number of observation points of a regular grid in ROI. The criteria are shown as follows:

a) To verify the homogeneity of the electric field strength, for over 75% of all the calculated points, the intended primary electric field strength  $E_{pri_i}$  which aligns the direction of the *co-polarization* at the tested point ( $P_i$ ) in ROI shall fulfil the following constraint Equation (1):

$$|E_{pri_i} \text{ (dBv)} - \bar{E}_{pri} \text{ (dBv)}| \leq \frac{Margin}{2} \text{ (dB)} \quad (1)$$

where *Margin* is the maximum tolerances of electric field variations and chosen to be 6 dB, and the mean value  $\bar{E}_{pri}$  of the  $N$  test points' electric field strength  $E_{pri_i}$  is calculated in Equation (2):

$$\bar{E}_{pri} \text{ (dBv)} = \frac{1}{N} \sum_{i=1}^N E_{pri_i} \text{ (dBv)} \quad (2)$$

Then using Equation (2), the standard deviation for the primary electric field of  $N$  test points can be calculated in Equation (3):

$$\sigma_{pri} \text{ (dB)} = \sqrt{\frac{1}{N-1} \sum_{i=1}^N (E_{pri_i} \text{ (dBv)} - \bar{E}_{pri} \text{ (dBv)})^2} \quad (3)$$

Assuming a normal distribution for the electric field strength, the probability fulfilling Equation (1) in  $N$  test points will fall in the range in statistical sense as expressed in constraint Equation (4):

$$|E_{pri_i} \text{ (dBv)} - \bar{E}_{pri} \text{ (dBv)}| \leq K \cdot \sigma_{pri} \quad (4)$$

where  $K$  is the factor of the confidence interval.

Following Equations (1) and (4), the calculated standard deviation should fulfill constraint Equation (5) in statistical sense:

$$\sigma_{pri} \leq \frac{Margin}{2 \times K} \quad (5)$$

b) To verify the TEM mode, the magnitudes of both secondary electric field components  $E_{sec_i}$  which are orthogonal to the direction of the *co-polarization* at the tested point ( $P_i$ ) in ROI, the unintended

field strengths should be at least 6 dB less than the primary component of the electric field  $E_{pri_i}$ , the intended field strength, over at least 75% of all tested points ( $P_i$ ) in ROI as shown in the following Equation (6):

$$E_{sec_i} \text{ (dBv)} - E_{pri_i} \text{ (dBv)} \leq -Margin \text{ (dB)} \tag{6}$$

where *Margin* is the maximum tolerance of electric field variations and chosen to be -6 dB.

In statistical sense for the normal distribution for the electric field strength of  $N$  test points, the probability fulfilling Equation (6) in the  $N$  test points will fall in the range expressed in Equation (7):

$$\bar{E}_{\frac{sec}{pri}} \text{ (dB)} + K \cdot \sigma_{\frac{sec}{pri}} \leq -Margin \text{ (dB)} \tag{7}$$

where factor  $K$  of the confidence interval is chosen to be 1.15 when the probability is 75%, and the mean value  $\bar{E}_{\frac{sec}{pri}}$  of  $N$  test points is calculated by Equation (8):

$$\bar{E}_{\frac{sec}{pri}} \text{ (dBv)} = \frac{1}{N} \sum_{i=1}^N (E_{sec_i} \text{ (dBv)} - E_{pri_i} \text{ (dBv)}) \tag{8}$$

and the standard deviation  $\sigma_{\frac{sec}{pri}}$  is calculated by Equation (9):

$$\sigma_{\frac{sec}{pri}} \text{ (dB)} = \sqrt{\frac{1}{N-1} \sum_{i=1}^N [(E_{sec_i} \text{ (dBv)} - E_{pri_i} \text{ (dBv)}) - \bar{E}_{\frac{sec}{pri}}]^2} \tag{9}$$

Following Equation (7), the standard deviation should fulfill constraint Equation (10):

$$\sigma_{\frac{sec}{pri}} \leq \frac{1}{K} (-Margin - \bar{E}_{\frac{sec}{pri}}) \tag{10}$$

As discussed above, the field uniformity criteria according to IEC 61000-4-20 can be expressed in constraint Equation (11):

$$\begin{cases} \sigma_{\frac{sec}{pri}} \leq \frac{1}{1.15} \times (-6 - \bar{E}_{\frac{sec}{pri}}) \\ \sigma_{pri} \leq \left( \frac{6}{2 \times 1.15} = 2.61 \right) \end{cases} \tag{11}$$

where *Margin* is chosen to be 6 dB and  $K$  chosen to be 1.15 when the probability is 75% to fulfill Equations (5) and (10).

As a result, the aperture field uniformity can be numerically analyzed by constraint Equation (11) when electromagnetic wave radiates from the aperture antenna in the design for exposure setups for biological experiments.

### 3. APERTURE-FIELD METHOD

To produce the required uniform plane electromagnetic wave with known operating frequencies, the aperture antenna is usually positioned in the exposure setup where the biological examples are exposed to RF. The analytical model where the aperture field distribution is analyzed for uniformity in ROI is shown in Figure 1.

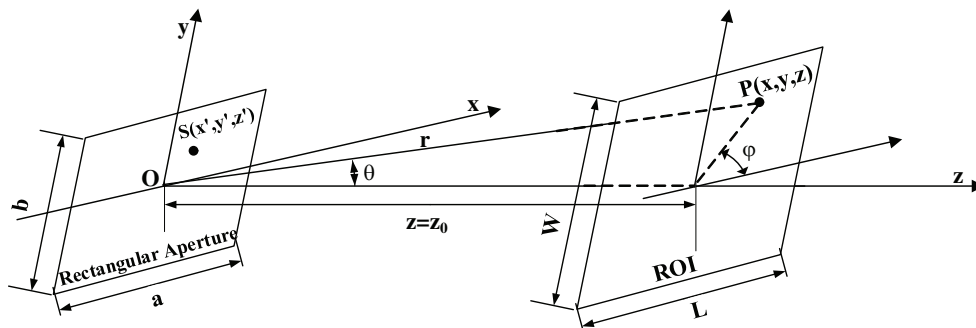


Figure 1. The analytical model on the aperture field.

### 3.1. ROI in the Aperture Field

In Figure 1, the analytical model consists of two parts: a rectangular aperture, which is the aperture antenna radiating the electromagnetic wave into free space, and the ROI, where  $E$ -field uniformity is required in biological experiments for RF exposure *in vivo* and *in vitro*. The rectangular aperture of geometry dimensions  $a$  along  $x$  and  $b$  along  $y$  is parallel to  $xoy$  plane and in  $z = 0$  plane, and the ROI of geometry dimensions  $L$  along  $x$  and  $W$  along  $y$  is parallel to the aperture plane and in  $z = z_0$  plane. The center of the rectangular aperture is at the coordinate origin, and the center of the ROI is at the point  $(0, 0, z_0)$ . The distance ( $z = z_0$ ) between the aperture antenna and ROI along  $z$  is the key factor to influence the field uniformity in ROI.

The aperture fields become the sources of the radiated field in ROI, and the geometrical representation of any chosen source point may be represented as a point  $S(x', y', z')$  in the aperture where  $z' = 0$  and

$$-\frac{a}{2} \leq x' \leq \frac{a}{2}, \quad -\frac{b}{2} \leq y' \leq \frac{b}{2}$$

To calculate the field distribution and uniformity in ROI, any observation point in ROI can be chosen, and the observation point may be represented as a point  $P(r, \theta, \varphi)$  in the spherical coordinates system or  $P(x, y, z)$  in the Cartesian coordinates system where  $z = z_0$  and

$$-\frac{L}{2} \leq x \leq \frac{L}{2}, \quad -\frac{H}{2} \leq y \leq \frac{H}{2}$$

In Figure 1 the ROI is generally located in the far field of aperture field and should satisfy the far-field conditions as:

$$z \geq \frac{2D^2}{\lambda} \quad (D^2 = a^2 + b^2)$$

where  $\lambda$  is wavelength of the operating frequency, and  $D$  is the typical size of the aperture.

### 3.2. Aperture-Field Method in Cartesian Coordinates System

As shown in Figure 1, any observation point  $P(x, y, z)$  inside the ROI can be selected, and the field of the point, radiated by the aperture sources, can be calculated by Aperture-Field Method (AFM) [13, 14]. If the aperture is fed by a rectangular waveguide, the primary  $E$ -field in the rectangular aperture is TE<sub>10</sub> mode in the  $y$  direction and is given by:

$$\vec{E}_a = \hat{a}_y E_0 \cos \frac{\pi x'}{a} \quad (12)$$

With Love's *equivalence principle* which replaces an actual radiating source by an equivalent source, the RF far field at any observation point  $P(r, \theta, \varphi)$  in the ROI is derived with  $\vec{E}_a$  in Equation (12) and expressed in the spherical coordinates system as follow:

$$\vec{E}_p = \hat{a}_r E_r + \hat{a}_\theta E_\theta + \hat{a}_\varphi E_\varphi \quad (13)$$

where

$$\begin{aligned} E_r &\cong 0 \\ E_\theta &= \frac{jk}{4\pi r} e^{-jkr} E_0 (1 + \cos \theta) \sin \varphi \int_s ds' \\ E_\varphi &= \frac{jk}{4\pi r} e^{-jkr} E_0 (1 + \cos \theta) \cos \varphi \int_s ds' \\ \int_s ds' &= \int_{-\frac{b}{2}}^{\frac{b}{2}} dy' \int_{-\frac{a}{2}}^{\frac{a}{2}} \cos \frac{\pi x'}{a} e^{jk(x' \sin \theta \cos \varphi + y' \sin \theta \sin \varphi)} dx' \end{aligned} \quad (14)$$

$k$  is the wavenumber and  $k = 2\pi/\lambda$ , and  $E_0$  is given in Equation (12).

Using Equations (13) and (14), the  $E$ -field of ROI in Cartesian coordinates system can be obtained as shown in Equation (15). In Equation (15),  $E_y$  is the primary component of the  $E$ -field aligned with

the intended polarization in the experiments, and  $E_x$  and  $E_z$  are unintended secondary components of the  $E$ -field and orthogonal to the primary field component, then they are orthogonal to each other in the Cartesian coordinate system. Referring to IEC 61000-4-20:2010, the field distribution of ROI can be analyzed using the following Equation (15).

$$\begin{aligned}\vec{E}_p &= \hat{a}_x E_x + \hat{a}_y E_y + \hat{a}_z E_z \\ E_x &= \frac{jk}{4\pi r} e^{-jkr} E_0 (\cos^2 \theta - 1) \sin \varphi \cos \varphi \int_s ds' \\ E_y &= \frac{jk}{4\pi r} e^{-jkr} E_0 (1 + \cos \theta) (\cos \theta \sin^2 \varphi + \cos^2 \varphi) \int_s ds' \\ E_z &= -\frac{jk}{4\pi r} e^{-jkr} E_0 (1 + \cos \theta) \sin \theta \sin \varphi \int_s ds'\end{aligned}\quad (15)$$

#### 4. ANALYSIS OF FIELD UNIFORMITY

According to IEC 61000-4-20:2010, we can analyze the field uniformity of ROI in the aperture field applying numerical AFM.

##### 4.1. Analysis of Field Uniformity Criteria Applying AFM

In the test for field uniformity, the electric field strength is measured at a given number of measurement points in the ROI according to IEC 61000-4-20:2010. The measurement points in a regular grid and space should be equal or less than 0.5 m. Applying AFM to analyze the field uniformity numerically, the rectangular ROI can be discretized into a regular grid along  $x$  and  $y$  whose intersection points are represented as observation point  $p(x_i, y_i, z_i)$ .  $E_x(x_i, y_i, z_i)$ ,  $E_y(x_i, y_i, z_i)$  and  $E_z(x_i, y_i, z_i)$  about  $E$ -field of the observation point  $p(x_i, y_i, z_i)$  can be calculated by Equation (15) in the Cartesian coordinate system. The intended  $E_y(x_i, y_i, z_i)$  is the magnitude of the primary electric field, and the unintended strengths,  $E_x(x_i, y_i, z_i)$  and  $E_z(x_i, y_i, z_i)$ , are the magnitudes of two secondary electric fields.

Following Equation (11) on the field uniformity criteria according to IEC 61000-4-20, the electric field in ROI is uniform when constraint Equation (16) is obeyed for all observation points according to IEC 61000-4-20:

$$\begin{cases} \sigma_{\frac{x}{y}} \leq \frac{1}{1.15} \cdot (-6 - \bar{E}_{\frac{x}{y}}) & (16a) \\ \sigma_{\frac{z}{y}} \leq \frac{1}{1.15} \cdot (-6 - \bar{E}_{\frac{z}{y}}) & (16b) \\ \sigma_y \leq 2.61 & (16c) \end{cases}$$

where  $\sigma_y$ , standard deviation of the magnitudes about the primary components of the electric field at observation points, is calculated by Equation (3). In Equation (16),  $\bar{E}_{\frac{x}{y}}$ ,  $\sigma_{\frac{x}{y}}$  which are the mean value and standard deviation of the  $E_x(x_i, y_i, z_i)$  to  $E_y(x_i, y_i, z_i)$  ratio at all observation points, and  $\bar{E}_{\frac{z}{y}}$ ,  $\sigma_{\frac{z}{y}}$  which are the mean value and standard deviation of the  $E_z(x_i, y_i, z_i)$  to  $E_y(x_i, y_i, z_i)$  ratio at all observation points, are calculated by Equations (8) and (9).

##### 4.2. Numerical Analysis of Field Uniformity in ROI

If the exposure setup for RF exposure experiments is modeled as shown in Figure 1, a numerical analysis on the field uniformity of ROI in the analytical model can be performed by applying numerical AFM to calculate the electric fields of ROI, and then, the field uniformity of the electric fields can be evaluated according to constraint Equation (16). In order to evaluate the field uniformity numerically, the software applying AFM and IEC61000-4-20:2010 standard should be designed appropriately. The software has two kinds of functions as shown in Figure 2.

Function I is applied to analyze the field uniformity of ROI with given dimensions of aperture and ROI, operating frequency and distance of ROI along  $z$  far from aperture. When Function I is selected,

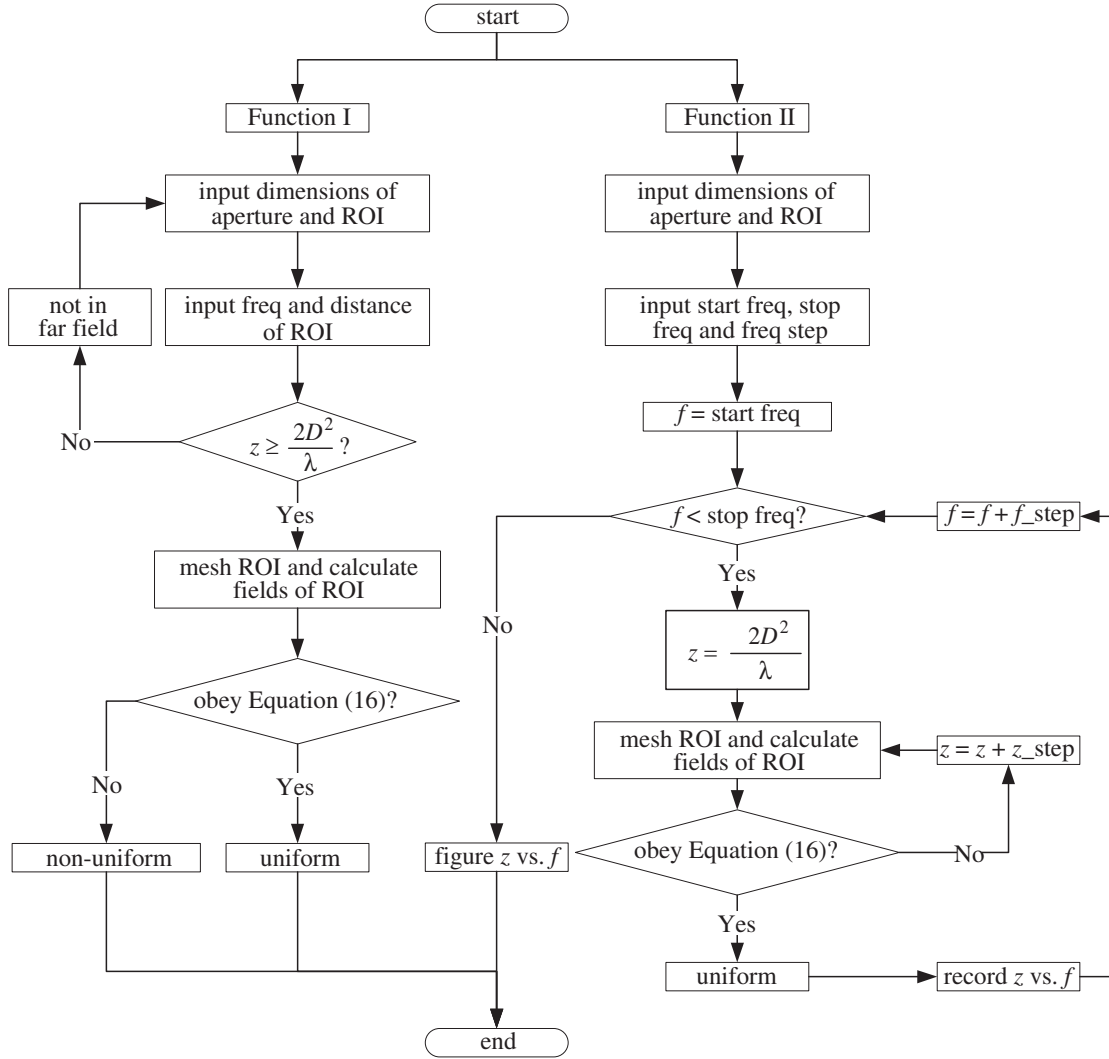


**Figure 2.** The diagram about numerical analysis of field uniformity in ROI.

we can input parameters about dimensions of aperture and ROI, the distance between the aperture and ROI along  $z$  as shown in Figure 1, with operating frequency first. Then, the distance along  $z$  can be verified whether or not in the far field according to far-field conditions. If the distance ( $z$ ) obeys the criteria of far field, the ROI is discretized into some observation points, and the fields are calculated by Equation (15). For all of the observation points, the constraint Equation (16) is given to evaluate the field uniformity of ROI with given parameters. Finally, the evaluation result, that the field is uniform or non-uniform, is displayed to the users.

Function II is designed to find the relationship between the field uniformity and given parameters with the dimensions of aperture and ROI, operating frequencies and the distance between the aperture and ROI. Then some parameters are not the same as Functions I. With given dimensions of aperture and ROI, operating frequency band with start and stop frequencies, the incremental frequency step and the incremental step of distance, and the minimum uniform distances vs. operating frequencies can be searched from the position ( $z = 2D^2/\lambda$ ) along  $z$  in the far field that is the nearest intended position obeying constraint Equation (16). If the field at the current position is not uniform vs. the current frequency, the routine with incremental step of distance can perform a loop call to search the uniform distance. Next, incrementing a given step to the current frequency, the routines are called again to find the minimum uniform distance vs. the current frequency until the current frequency is out of operating frequency band. Finally, the minimum uniform distances vs. frequencies are identified.

### 4.3. Application of Field Uniformity Analysis

For a given WR-430 rectangular open-ended waveguide whose operating frequency band is from 1.7 GHz to 2.6 GHz, and dimensions are 109.22 mm × 54.61 mm, the case of field uniformity analysis is applied by Function I and Function II as shown in Figure 2. The ROI (466 mm × 315 mm) is meshed with 32 × 32 regular grids uniformly along each side where the cage (466 mm × 315 mm × 210 mm) houses experimental mice. If the position of ROI along  $z$  is  $z = 300$  mm far from the WR-430 waveguide aperture as shown in Figure 1 and the given operating frequency is 1800 MHz, the field tested by Function I is uniform according to constraint Equation (16) recommended by IEC61000-4-20:2010. However, the result of field uniformity does not obey Equation (16) if the input parameter about the distance of ROI along  $z$  is changed to  $z = 270$  mm. Performing Function II, the relationship between minimum uniform distances and frequencies are figured in Figure 3 with the given aperture and ROI.

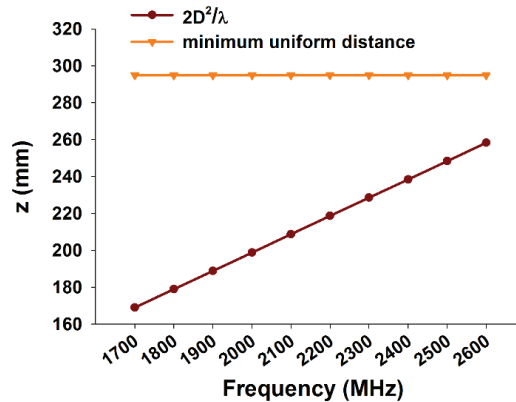


Figure 3. Minimum uniform distances vs. frequencies.

In Figure 3, it is clear that the minimum uniform distances are further than the threshold of far field ( $z = 2D^2/\lambda$ ) at all points of operating frequencies. Furthermore, the minimum distance is nearly unchanged in the whole operating band. When Function II is performed, Equations (16a) and (16c) are found to obey respectively if the distance ( $z$ ) is equal to or greater than the threshold of far field at every operating frequency. However, the distance should not be less than the minimum uniform distance in order to obey the constraint Equation (16b). Using Equations (8) and (15),  $E_{z/y}$  is expressed as follow:

$$E_{z/y}(\text{dB}) = 20 \log \frac{E_z}{E_y} = 20 \log \left( \frac{\sin \theta \sin \varphi}{\cos \theta \sin^2 \varphi + \cos^2 \varphi} \right) \quad (17)$$

therefore  $\sigma_{z/y}$  is correlated with the dimensions and distance of ROI and uncorrelated with frequencies so that the minimum uniform distance obeying constraint Equation (16b) is a nearly unchanged value.

With the given dimensions of aperture and ROI as shown in Figure 1, the operating frequency and minimum uniform distance can be obtained by Function II as shown in Figure 3. If the distance between the given aperture and ROI exceeds the minimum uniform distance to the operating frequency as in Figure 3, it is certain that the field in the ROI is uniform because the magnitudes of the primary  $E$ -field and both secondary  $E$ -field in the ROI fulfill Equation (16). Therefore, the position of the ROI can be designed according to the minimum uniform distance in Figure 3 given by Function II when the well-characterized exposure setup is designed with the field uniformity where the electromagnetic field is radiated by rectangular aperture antenna for biological experiments.

## 5. CONCLUSION

Field uniformity is very important in biological experiments using *in vitro* and/or *in vivo* RF exposure. In this paper, a numerical analysis and aperture field method according to IEC 61000-4-20:2010 standard are described to ascertain the field uniformity in biological experiments. Two functions evaluating field

uniformity of ROI are studied, and a case about WR-430 rectangular open-ended waveguide is analyzed whether or not the field is uniform in the ROI. The minimum uniform distances vs. frequencies for the given the dimensions of aperture and ROI are proposed which may be a constraint condition to design RF exposure setups.

## ACKNOWLEDGMENT

This work was funded in part by the National Natural Science Foundation of China (81773463) and in part by the interdisciplinary pre-research program of Soochow University.

## REFERENCES

1. Kim, J. and Y. Rahmat-Samii, "Implanted antennas inside a human body simulations, designs, and characterizations," *IEEE Trans. Microw. Theory Tech.* Vol. 52, 1934–1943, Aug. 2004.
2. Xia, W., K. Saito, M. Takahashi, and K. Ito, "Performances of an implanted cavity slot antenna embedded in the human arm," *IEEE Trans. Antennas Propagat.*, Vol. 57, 894–899, Apr. 2009.
3. Liu, C., Y. X. Guo, H. Sun, and S. Xiao, "Design and safety considerations of an implantable rectenna for far-field wireless power transfer," *IEEE Trans. Antennas Propagat.*, Vol. 62, 5798–5806, Aug. 2014.
4. Miquel, A. G., S. Curto, N. Vidal, J. M. Lopez-Villegas, F. M. Ramos, and P. Prakash, "Multilayered broadband antenna for compact embedded implantable medical devices: Design and characterization," *Progress In Electromagnetics Research*, Vol. 159, 1–13, Apr. 2017.
5. Sannino, A., M. L. Calabrese, G. D'Ambrosio, R. Massa, G. Petraglia, P. Mita, M. Sarti, and M. R. Sacrifscarfi, "Evaluation of cytotoxic and genotoxic effects in human peripheral blood leukocytes following exposure to 1950-MHz modulated signal," *IEEE Trans. Plasma Sci.* Vol. 34, 1331–1448, Aug. 2006.
6. Adan, D., C. Remacl, and A. V. Vorst, "Results of a long-term low-level microwave exposure of rats," *IEEE Trans. Microw. Theory Tech.* Vol. 57, 2488–2497, Sep. 2009.
7. Qin, F., J. Zhang, H. Cao, W. Guo, L. Chen, O. Shen, J. Sun, Y. Cao, J. Wang, and J. Tong, "Circadian alterations of reproductive functional markers in male rats exposed to 1800 MHz radiofrequency field," *Chronobiol. Int.*, Vol. 31, 123–133, Jan. 2013.
8. Kwon, M. S. and H. Hämäläinen, "Effects of mobile phone electromagnetic fields: Critical evaluation of behavioral and neurophysiological studies," *Bioelectromagnetics*, Vol. 32, 253–272, Dec. 2011.
9. Paffi, A., F. Apollonio, G. A. Lovisolo, C. Marino, R. Pinto, M. Repacholi, and M. Liberti, "Considerations for developing an RF exposure system: A review for in vitro biological experiments," *IEEE Trans. Antennas Propagat.*, Vol. 58, 2702–2714, Oct. 2010.
10. Calabrese, M. L., G. d'Ambrosio, R. Massa, and G. Petraglia, "A high efficiency waveguide applicator for in vitro exposure of mammalian cells at 1.95 GHz," *IEEE Trans. Microw. Theory Techn.*, Vol. 54, 2256–2262, May 2006.
11. Romeo, S., C. D'Avino, D. Pinchera, O. Zeni, M. R. Scarfi, and R. Massa, "A waveguide applicator for *In Vitro* exposures to single or multiple ICT frequencies," *IEEE Trans. Microw. Theory Tech.* Vol. 61, 1994–2004, May 2013.
12. IEC 61000-4-20, "Electromagnetic compatibility (EMC) — Part 4: Testing and measurement techniques, Section 20: Emission and immunity testing in transverse electromagnetic (TEM) waveguides," *International Electrotechnical Commission*, 2010.
13. Zhong, S., *Antenna Theory and Technoiques*, Publishing House of Electronics Industry, Beijing, 2011.
14. Silver, S., *Microwave Antenna Theory and Design*, McGraw-Hill Book Co, London, 2008.